



1 **Effect of mixing structure on the water uptake of mixtures of**
2 **ammonium sulfate and phthalic acid particles**

3 Weigang Wang^{1,4†}, Ting Lei^{2,3†}, Andreas Zuend⁵, Hang Su³, Yafang Cheng², Yajun Shi¹,
4 Maofa Ge^{1,4,6}, Mingyuan Liu^{1,4}

5 ¹State Key Laboratory for Structural Chemistry of Unstable and Stable Species, Beijing National
6 Laboratory for Molecular Sciences (BNLMS), CAS Research/Education Center for Excellence in
7 Molecular Sciences, Institute of Chemistry, Chinese Academy of Sciences, Beijing 100190, P. R. China

8 ²Minerva Research Group, Max Planck Institute for Chemistry, Mainz 55128, Germany

9 ³Multiphase Chemistry Department, Max Planck Institute for Chemistry, Mainz 55128, Germany

10 ⁴University of Chinese Academy of Sciences, Beijing 100049, PR China

11 ⁵Department of Atmospheric and Oceanic Sciences, McGill University, Montreal, Quebec, Canada

12 ⁶Center for Excellence in Regional Atmospheric Environment, Institute of Urban Environment, Chinese
13 Academy of Sciences, Xiamen 361021, PR China

14 † These authors contributed equally to this work

15 Correspondence to: Weigang Wang (wangwg@iccas.ac.cn) and Maofa Ge (gemaofa@iccas.ac.cn)

16

17 **Abstract.** Aerosol mixing state regulates the interactions between water molecules and particles
18 and thus controls the aerosol activation and hygroscopic growth, which thereby influences the
19 visibility degradation, cloud formation, and its radiative forcing. Current studies on the mixing
20 structure effects on aerosol hygroscopicity, however, is few reported. Here we investigated the effect
21 of phthalic acid (PA) coatings on the hygroscopic behavior of the core-shell mixtures of ammonium
22 sulfate (AS) with PA using a coating-hygroscopicity tandem differential mobility analyzer (coating-
23 HTDMA). The slow increase in the hygroscopic growth factor of core-shell particles is observed



24 with increasing thickness of coating PA prior to the DRH of AS. At RH above 80 %, a decrease in
25 hygroscopic growth factor of particles occurs as the thickness of PA shell increases, which indicates
26 that the increase of PA mass fractions leads to a reduction of the overall core-shell particle
27 hygroscopicity. In addition, the use of the ZSR relation leads to the underestimation for the measured
28 growth factors of core-shell particles without consideration of the morphological effect of core-shell
29 particles. For the AS/PA well mixed particles, a shift of deliquescence relative humidity (DRH) of
30 AS to lower relative humidity (RH) is observed due to the presence of PA in the well-mixed particles.
31 The predicted hygroscopic growth factor using the ZSR relation is consistent with the measured
32 hygroscopic growth factor of the well-mixed particles. Moreover, we compared and discussed the
33 influence of mixing states on the water uptake of AS/PA aerosol particles. It is found that the
34 hygroscopic growth factor of the core-shell particles is slightly higher than that of the well-mixed
35 particles with the same mass fractions of PA at RH above 80%. For our observation of AS/PA
36 particles may contribute to a growing field of knowledge regarding the influence of coating
37 properties and mixing structure on water uptake.

38

39 **1 Introduction**

40 The ability of aerosol particles to absorb and maintain water molecules, called hygroscopicity, is
41 one of the most important physico-chemical properties of atmospheric aerosol particles with
42 profound implications (Shi et al., 2012; Lei et al., 2014, 2018; Gupta et al., 2015; Hodas et al., et
43 al., 2015; Zawadowicz et al., 2015; Martin et al., 2017). It might determine the phase state (Mu et
44 al., 2018), size (Peng et al., 2001; Choi et al., 2002), mixing state, optical properties, and chemical
45 reactivity of atmospheric aerosols exposed to the environment of the different relative humidities



46 (Heintzenberg et al., 2001; Rudich et al., 2003; Spindler et al., 2007; Abo Riziq et al., 2007, 2008;
47 Eichler et al., 2008). Moreover, the change of these properties after water absorption on aerosol
48 particles can strongly affect the cloud formation, aerosol radiative forcing, global climate, and even
49 human health (Cheng et al., 2008; Reutter et al., 2009; Rose et al., 2011; Stock et al., 2011; Liu et
50 al., 2012, 2013; Tie et al., 2017). Therefore, the interaction between water molecules and aerosol
51 particles is crucial for a better understanding of the aerosol-cloud-climate effects in the atmosphere
52 (Sjogren et al., 2007; Zamora et al., 2011; Jing et al., 2016).

53 Atmospheric aerosols contain a complex mixture of inorganic and organic compounds in the
54 different mixing structures, e.g., externally mixed, internally mixed (Ganguly et al., 2006). The
55 internally mixed aerosol particles may be divided into homogeneous and heterogeneous internally
56 mixed aerosol particles (Lang-Yona et al., 2009), which could, in turn, strongly influence the water
57 uptake, optical properties, and the cloud condensation nuclei (CCN) ability of the particles (Lesins
58 et al., 2002; Falkovich et al., 2004; Zhang et al., 2005; Schwarz et al., 2006; Su et al., 2010). Most
59 of earlier studies on the hygroscopic behavior of multi-components aerosol focus on the well mixed
60 particles generated from homogeneously internally mixed solutions (Miñambres et al., 2010; Shi et
61 al., 2014; Gupta et al., 2015; Jing et al., 2016; Lei et al., 2014; 2018) For example, Choi and Chan
62 (2002) studied on the effects of glycerol, succinic acid, malonic acid, citric acid, and glutaric acid
63 on the hygroscopic properties of sodium chloride and AS in the well mixed aerosol particles,
64 respectively using an electrodynamic balance. They observed that the deliquescence and
65 efflorescence of sodium chloride and AS were affected by the presence of different organic
66 components in the mixed aerosol particles. Concerning the hygroscopicity of the heterogeneity of
67 internally mixed aerosol particles, such as core-shell particles, there are several studies on



68 investigating their interaction with water molecules (Ciobanu et al., 2009; Song et al., 2012;
69 Shiraiwa et al., 2013; Hodas et al., 2015; Song et al., 2018). However, to date, few laboratory studies
70 on the influence of organic coatings on the hygroscopic behavior of seed particles and the difference
71 of mixing state effects on the hygroscopicity of aerosol particles (Zhang et al., 2008; Pagels et al.,
72 2009; Xue et al., 2009; Lang-Yona et al., 2010; Ditas et al., 2018). E.g., A HTDMA study on the
73 organic coating effects on the hygroscopicity of AS core was studied by Maskey et al. (2014). They
74 observed a shift of DRH of AS to lower RH for the core-shell particles due to presence of
75 levoglucosan coatings. They further compared water absorption on AS/levoglucosan core-shell
76 particles and the AS/succinic acid core-shell particles. They suggests that difference organic
77 coatings lead to changes in the hygroscopic properties of core-shell particles. Chan et al. (2006)
78 investigated hygroscopicity of AS coated with different mass fractions of glutaric acid during two
79 continuous humidification and dehumidification cycles using a Raman spectra and an
80 electrodynamic balance. They observed different hygroscopic behavior and morphology of aerosol
81 particles between the two humidification and dehumidification cycles due to the different mixing
82 states. Therefore, to investigate organic coating effect on the hygroscopicity of seed aerosol particles
83 and further to study on difference of mixing states effects on the hygroscopic behavior of aerosol
84 particles are crucial for estimation the direct and indirect radiative effect of aerosol particles on the
85 Earth's climate (Saxena et al., 1995; Ansari et al., 2000; Maskey et al., 2014).

86 PA is ubiquitous in rural mountains and marine atmosphere in Asia (Wang et al., 2011). It is mainly
87 produced by the photo-oxidation of volatile organic compounds (VOCs), such as xylene, and
88 naphthalene (Kawamura and Ikushima, 1993; Schauer et al., 1996; Zhang et al., 2016). PA has also
89 been identified as a significant contributor to the urban organic compounds (Rogge et al., 1993). PA



90 particles are generally used as a tracer for the secondary organic aerosol (SOA) in atmospheric fine
91 particles (Schauer et al., 2000, 2002). Recently, Zhang et al. (2016) reported the importance of
92 atmospheric PA aerosol particles in the visibility degradation and the formation of CCN. The organic
93 PA can have profound effect on light scattering, hygroscopicity, and phase transition properties of
94 multicomponent atmospheric aerosols. However, these physico-chemical properties of PA have
95 been little documented in the literature (Brooks et al., 2004; Liu et al., 2016). Here we summarized
96 a few studies on the hygroscopicity of the PA-containing aerosol particles. Brooks et al. (2004)
97 investigated continuous hygroscopic growth of PA aerosol particles in the humidification process
98 using a HTDMA technique. Hori et al. (2003) and Huff Hartz et al. (2006) measured the high CCN
99 activity of PA in spite of its low solubility. Also, the liquid-liquid phase separations (LLPS) with
100 aerosol particles consisting organic and inorganic components were observed by many groups
101 (Ciobanu et al., 2009; Betram et al., 2011; Song et al. 2012a, 2012b; You et al., 2014). For example,
102 Song et al. (2012a, 2012b) investigated that LLPS occurs in the mixed dicarboxylic acids containing
103 5, 6, and 7 carbon using an optical microscopy and micro-Raman spectroscopy, and further
104 established that occurrence of LLPS of aerosol particles has an average elemental oxygen-to-carbon
105 (O:C) ratio of the organic fraction of less than 0.8. Subsequently, the occurrence of liquid-liquid
106 phase separation in the internally mixed aerosols consisting of AS and PA was performed by Zhou
107 et al. (2014) during the dehumidification processes using the Raman spectra. You et al. (2014)
108 further found that the LLPS of aerosol particles with a different O: C ratio of $0.5 < O: C < 0.8$ depends
109 on the types of organic functional groups and inorganic salts presented. Therefore, these studies
110 suggest that the LLPS in the mixed organic and inorganic components aerosol particles is influenced
111 by the amounts of organic and inorganic aerosol components and types.



112 In this work, we investigated the effect of the different thickness of coating PA and the core size on
113 the water uptake of core-shell particles containing AS, and further studied the effect of the mixing
114 states on the hygroscopic behavior of PA /AS aerosol particles using a HTDMA technique. For
115 example, we compared the hygroscopic behavior of well-mixed AS/PA particles with that of core-
116 shell AS/PA particles with the same PA mass fractions. In addition, we used the Zdanovskii-Stokes-
117 Robinson (ZSR) relation and the Aerosol Inorganic-Organic Mixtures Functional groups Activity
118 Coefficients (AIOMFAC) model (Zuend et al., 2008; 2011) to predict the hygroscopic growth factor
119 (GF) of mixed aerosol particles in the different mixing structure. Moreover, the AIOMFAC-based
120 model with a version of the liquid-liquid equilibrium (LLE) algorithm was employed in our study
121 to predict the phase compositions of liquid and solid phases for a given composition of a mixture
122 (Zuend and Seinfeld, 2013).

123

124 **2 Experimental and modeling methods**

125 **2.1 HTDMA setup and experimental protocol**

126 A HTDMA setup is employed to measure the aerosol nanoparticle hygroscopic growth factor (g_f)
127 and phase transition in the RH range from 5% to 90 %. Here, g_f is defined as the ratio of mobility
128 diameter of aerosol particles after humidification ($D_m(\text{RH})$) to that dry condition ($D_m(<5\% \text{ RH})$).
129 Figure 1 shows a schematic diagram of the HTDMA setup. It is comprised of four main components,
130 including three differential mobility analyzers (DMA), a condensation particle counter (CPC), a
131 humidification system, and a coating system. The more detail information on the HTDMA setup,
132 calibration, and verification have been described elsewhere (Lei et al., 2014; 2018; Jing et al., 2016;
133 Liu et al., 2016). In our study, the particle-sizing, the aerosol/sheath flow rates, and DMA voltage



134 supply have been calibrated every month, respectively. The uncertainty of aerosol/sheath flow rates
135 are kept within $\pm 1\%$ around the reference values. The deviations of the measured DMAs voltage
136 from set-point values is less than $\pm 1\%$. The sizing agreement of DMAs between measured diameter
137 of polystyrene latex (PSL) spheres and their nominal diameter (100 ± 3 nm) is within $\pm 1\%$. The
138 chemical substances and related to physical properties are available in the Supporting Information
139 Table S1. The solutions used in our measurements are prepared with distilled and de-ionized millo-
140 Q water (resistivity of 18.2 M Ω cm at 298 K).

141 **2.1.1 Homogeneously internally mixed AS/PA Aerosol particles**

142 Briefly, poly-disperse aerosol particles were atomized from homogeneous bulk solutions with
143 different mass fractions of PA and AS (Fig. 1), assuming that the compositions of aerosol particles
144 remain the same as that of the solutions used in the atomizer (MSP 1500, MSP). The resulting
145 particles were dried and subsequently charged through a dryer and then a neutralizer, respectively.
146 A mono-disperse distribution of particles with a desired diameter were selected by the first
147 differential mobility analyzer (DMA1) with RH below 5% . After particle sizing, the aerosol
148 particles were exposed to a humidification mode ($5\% \rightarrow 90\%$) in the Nafion conditioner tubes. The
149 number size distributions of humidified aerosol particles were then measured by a DMA3 coupled
150 with a CPC. To have a precise control of the aerosol RH, the flow rates of the humid and dry air
151 were adjusted with a proportional-integral-derivative (PID) system. Also, to ensure the sufficient
152 water equilibrium with aerosol particles, the difference between RH2 and RH3 (RH in the sheath
153 flow) was within 2% during the experiment.

154 **2.1.2 Heterogeneously internally mixed AS/PA aerosol aerosols**

155 The seed aerosol particles were generated from an aqueous solution of AS (0.05 wt%) by an atomizer.



156 After a passage through a silica gel diffusion dryer and a neutralizer, the seed aerosol particles with
157 a certain diameter (100, 150, 200nm, respectively) were firstly selected by a DMA1 and then
158 exposed to organic vapors in a coating system. To be specific, the coating system contains a
159 controlled silicone oil bath vaporizer, a reservoir of organic compound, and a condenser. The seed
160 AS particles passed through a sealed flask immersed in a silicone oil bath. The sealed flask was
161 filled with the PA powder. The PA vapors were enriched into the aerosol flow by heating. The
162 resulting organic vapors were condensed onto the seed particles after cooling to an ambient
163 environment through a condenser. Similarly, this system for coating organic components on the
164 particles has been proved to be efficient by Abo Riziq et al. (2008). The coated particles of certain
165 sizes were then selected by the DMA2 to determine the thickness of organic components ($D_{\text{total}} =$
166 $D_{\text{core}} + \text{coating}$). After core-shell particle-sizing, aerosols pre-humidified in a Nafion tube and flowed
167 into the second Nafion humidifier at the set RH2 to reach equilibrium at the RH condition. Finally,
168 the conditioning core-shell particle was detected by a DMA3 and a CPC at ambient temperature.
169 The uncertainty of thickness of coating PA was ± 1.0 nm, considering the fluctuation in temperature
170 and uncertainty of sizing measurements by DMAs.

171 2.2 Theory and modeling methods

172 2.2.1 GF data fit

173 We use the following expression to predict the hygroscopic growth factor of individual components.

$$174 \quad GF = \left[1 + (a + b * a_w + c * a_w^2) \frac{a_w}{1-a_w} \right]^{\frac{1}{3}} \quad (1)$$

175 Here it is assumed that water activity (a_w) is equal to the water saturation ratio ($a_w = RH / 100$ %).

176 The coefficients a, b, and c are determined by fitting Eq. (1), and their values are shown in Table 1

177 according to the measured GF data against RH. The equation (1) is expected to fit the continuous



178 water uptake behavior of particles (Brooks et al., 2004; Kreidenweis et al., 2015).

179 2.2.2 GF predictions by ZSR

180 We use the Zdanovskii-Stokes-Robinson (ZSR) relation to calculate the hygroscopic growth factor
181 of mixed particles, GF_{mixed} . The GF of a mixture can be estimated from the GF_j of the pure
182 components j and their respective volume fractions, ϵ_j , in the mixture (Malm and Kreidenweis,
183 1997).

$$184 \quad GF_{mix} = \left[\sum_j \epsilon_j (GF_j)^3 \right]^{\frac{1}{3}} \quad (2)$$

$$185 \quad \epsilon_{AS} = \frac{\frac{4}{3}\pi R_{AS}^3}{\frac{4}{3}\pi R_{core-shell}^3} \quad (3)$$

186

187 3 Results and discussion

188 3.1 Hygroscopic growth of homogeneously internally mixed aerosol particles

189 Figure 2 shows the measured hygroscopic growth factors of the AS, PA, and well-mixed AS with
190 different mass fractions of PA particles with dry diameter 100nm against RH, respectively. During
191 the hydration mode, there is no change in size until a slow increase occurs at 60% RH in the case of
192 well-mixed AS/PA aerosol particles. This increase may occur because the PA uptakes a small amount
193 of water. However, an abrupt increase in the hygroscopic growth factor is observed at 75% RH for
194 well-mixed particles containing 50wt, 75wt % PA, of which the growth factor is higher than that of
195 pure PA aerosol particles (1.09 ± 0.01 nm from measurements shown in Fig. 2) at the same RH. An
196 interesting, yet contrasting phenomenon is that water uptake for well-mixed particles containing
197 50wt % PA components is relatively higher than that of mixtures containing 75wt % PA at 75% RH.
198 One possible reason is that the full deliquescence of AS in the well-mixed particles with 50wt % PA
199 components is completed at 75 % RH, while AS in the mixtures containing 75wt % PA components



200 is partially deliquescent. A decrease in the hygroscopic growth factor of well-mixed AS/PA particles
201 with increasing mass fractions of PA is observed at RH above 80 %. For example, the measured
202 growth factors for internal mixtures containing 25wt, 50wt, 75wt % PA are 1.36, 1.28, 1.19 at 80%
203 RH, respectively, lower than the growth factor of 1.45 for pure deliquesced AS particles (value from
204 measurements shown in Fig. 2) at the same RH. Also, the measured hygroscopic growth factors
205 within experimental uncertainty were in good agreement with the results from the well-mixed
206 particles performed by Hämeri et al. (2002). In addition, with increasing mass fractions of PA in the
207 well-mixed particles, the smoothing of the hygroscopic growth factor curves is obvious, indicating
208 that the PA aerosol particles have a significant effect on the water uptake of well-mixed AS/PA
209 particles such as a shift or suppression of DRH of AS in the mixed particles. For example, in the
210 case of 1:3 mixtures of AS:PA (by mass), 75wt% PA in the well-mixed particles suppresses the
211 deliquescence of AS, i.e., AS in the well-mixed particles slowly dissolve into the liquid phase due
212 to continuous water uptake of PA prior to the deliquescence relative humidity of AS (80% RH). This
213 similar phenomenon was observed by previous studies (e.g., Hämeri et al., 2002; Qiu and Zhang,
214 2013). For example, Qiu and Zhang (2013) observed that mixture particles consisting of
215 dimethylammonium sulfate and AS exhibited a moderate growth by water uptake in the RH range of
216 40%-70% RH. The calculated growth factors from a model based on the ZSR relation agree well
217 with the hygroscopic growth factors of well-mixed AS/PA particles when accounting for
218 measurement uncertainty. A possible reason for this good agreement is that the measured growth
219 factors referring to the water uptake contribution by PA in the ZSR relation are obtained from the
220 fitted growth curve of pure PA particles (as shown in Fig. 2. Fitted expression, Eq. (1)). Thus, in the
221 case of well-mixed AS/PA, relatively good agreement with the experimental growth factors of



222 mixtures with 25, 50, and 75 wt % PA demonstrates that individual components independently
223 absorb water in proportion to their volume. However, the discrepancy between measured growth
224 factor of well-mixed AS/PA particles at 75 % RH and the predicted growth factors by using the ZSR
225 relation may be due to the molecule interaction between organic molecular and completely or
226 partially dissolved AS ions. A similar phenomenon was reported for well-mixed mixtures of AS +
227 levoglucosan in the previous study by Lei et al (2014, 2018).

228 **3.2 Hygroscopic growth of core-shell structured aerosol particles**

229 Figure 3 shows the measured hygroscopic growth of core-shell structured particles as a function of
230 RH. Here, we investigated the hygroscopic behavior of samples of various seed particle sizes (AS
231 particle dry diameter of 100, 150, 200nm) and coating (PA coating of 10, 20, 30, 50nm), respectively.
232 The core-shell structured particles start to absorb a small amount of water at RH lower than the
233 DRH of AS due to the organic coating. A similar behavior has been observed for core-shell
234 structured particles containing AS and palmitic acid by Garland et al. (2005), where early water
235 uptake and reduced hygroscopic growth after deliquescence of AS (compared to pure AS aerosols)
236 were reported. A reduction of the hygroscopic growth factors of core-shell particles becomes
237 obvious as the thickness of the PA shell increases after the deliquescence of core-shell particles. For
238 example, the measured growth factor value at 80% RH is 1.45, 1.40, 1.32, and 1.28 for core-shell
239 particles containing 100nm AS and 10, 20, 30, 50nm coating PA shell, respectively. The kinetic
240 limitation on the core-shell particles is expected to increase considerably with increasing the
241 thickness of the coating PA shells, which retards the transport rate of water molecules across core-
242 shell aerosol particles/air interface. In addition, the measured hygroscopic growth factor of core-
243 shell AS/PA mixtures is predicted by the ZSR relation, which is based on the hygroscopic growth



244 factors of AS and PA derived from the E-AIM predictions for AS and the fitted GF curve (Eq. 1).
245 The ZSR-based predictions are lower than that of core-shell aerosol particles at RH in the range of
246 5-90%. The underprediction of the ZSR relation was also observed in the literatures (Chan et al.,
247 2006; Sjogren et al., 2007). Sjogren et al. (2006) observed a strong higher water uptake of mixtures
248 consisting of AS and adipic acid with different mass ratios (1:2, 1:3, and 1:4) at RH above 80 %
249 compared with ZSR relation in the hydration condition. They assumed that adipic acid is more likely
250 to enclose the water-soluble AS in veins and cavities, which results in easy uptake of water and a
251 negative curvature of the solution meniscus at the opening of the vein compared to a flat or convex
252 particle surface. Thence, in the case of AS/PA core-shell particles, one potential reason for the
253 underestimation of the measured growth factor by ZSR relation is the morphology effect on the
254 core-shell structured AS/PA particle. To be specific, for the core-shell aerosol particles consisting of
255 PA and AS, especially at 80% RH, it shows a considerable amount of water uptake due to the
256 dissolution of the AS core. This dissolution of AS may form completely or partially mixed AS/PA
257 solution droplets. The resulting effect of the arrangement and restructuring of core-shell structured
258 particles may change the hygroscopicity and mixing state of the core-shell particles at RH above
259 80% (Chan et al., 2006; Sjogren et al., 2007). Another morphological effect could be that
260 morphology of a somewhat porous polycrystalline AS core could lead to a larger amount of AS in
261 the particles at RH prior to deliquescence of AS – to appear as a 100-200 nm mobility diameter –
262 hence a thinner than 10-50 PA coating to bring it to a near spherical shape of 110-250 nm core-shell
263 particles (Zelenyuk et al., 2006).
264 Figure 4 shows that the experimental water absorption of the varying size of AS core coated with
265 50-nm PA shell in the hydration condition. In the case of 50nm-PA shell coated with a certain size



266 of the AS seed (100, 150, 200nm) with respect to 68wt, 55wt, 46 wt % PA in the core-shell particles,
267 It exhibits an increase in hygroscopic growth factor of core-shell particles at RH below 80 % as the
268 size of AS core decreases. However, a decrease in hygroscopic growth factor of core-shell mixtures
269 is observed at RH above 80 % with decreasing the size of the AS core. This indicates that the 50nm-
270 PA shell in the core-shell particles have predominantly contributed to the hygroscopic growth of
271 core-shell particles at low RH. At high RH (e.g., after AS deliquescence), however, 50-nm PA
272 coating shows a weak kinetic limitations for water uptake by core-shell particles as the size of AS
273 core increases. For example, the measured growth factor value is 1.28, 1.34, and 1.40 at 80% RH
274 for 100-200 nm AS core in the mixed particles, respectively. The discrepancy between measured
275 hygroscopic growth factors and predicted hygroscopic growth factors of core-shell particles by ZSR
276 relation, as discussed in Sect. 3.2, is due to the morphology effect. For ZSR prediction, it assumes
277 volume fraction of AS components is constant according to the ratio of volume of AS core in the
278 sphere to the volume of core-shell sphere based on Eq. (3). Without considering morphology effect,
279 the ZSR prediction results in an underestimation of hygroscopic growth factors of core-shell
280 particles.

281 **3.3 Comparison of heterogeneously and homogeneously internally mixed AS/PA aerosol** 282 **particles**

283 Figure 5 shows the hydration curves of different AS cores coated with the different mass fractions
284 of PA loading (shown in the Supporting Information Table S2) in comparison with those of the well-
285 mixed with the same PA mass fractions particles, pure AS particles, and pure PA particles in the
286 range of 5 – 90% RH. The effect of the coating PA on core-shell particles becomes more pronounced
287 than that of PA in the well-mixed particles at RH below 70% as shown in Fig 5a-b, which leads to



288 higher amounts of water absorption at low RH. However, compared to Fig 5a-b, Fig. 5c shows the
289 hygroscopic growth factors of well mixed AS/PA is slightly higher than that of AS/PA core-shell
290 particles with 46% wt PA. At 75% RH, the measured growth factor value of core-shell particles is
291 lower than that of homogeneously internally mixed mixtures in the PA mass fraction range from
292 68wt to 46wt % due to the mass transfer limitations of water vapor transport to the AS core in the
293 core-shell particles. For the well mixed AS/PA particles, however, partial dissolution of AS into the
294 liquid AP phase may lead to more water uptake by well mixed particles. For example, for the core-
295 shell mixtures with 68wt % PA loading, the experimental growth factor value is 1.09 at 75% RH,
296 relative to the growth factor of 1.17 of well-mixed mixtures AS/PA. After an abrupt increase in
297 particle diameter of mixed particles, the core-shell AS/PA particles uptake slightly more water than
298 well-mixed AS/PA with the same mass fractions of PA as RH increases above 80%. Core-shell
299 particle morphology may experience the restructuring and associate size change of particles. A
300 similar hygroscopic behavior was observed in previous papers (Chan et al., 2006; Sjogren et al.,
301 2007; Maskey et al., 2014). Chan et al. (2006) observed for hygroscopicity of 49wt % glutaric acid
302 coated on AS core during two continuous hydration cycles: the experimental growth factor of the
303 fresh core-shell of AS and glutaric acid in the first hydration cycle is a bit higher than those in second
304 hydration cycle with the same mass fractions of glutaric acid. They suggested that the mixing state
305 has changed from core-shell to well-mixed state during the humidification process. Also, a slightly
306 higher growth factor of core-shell particles than that of well-mixed particles was found when
307 comparing the hygroscopic growth factors of 49wt % glutaric acid coated on AS core with that of
308 well-mixed mixtures of AS with the same mass fractions of glutaric acid from different papers (Choi
309 et al., 2002; Chan et al., 2006). However, a contrasting observation was observed in the previous



310 study (Maskey et al., 2014). Maskey et al. (2014) investigated the hygroscopic behavior of the
311 internal mixtures consisting AS coated with either succinic acid or levoglucosan in the different
312 mixing state with the same volume fractions of organic compounds. The growth factor of core-shell
313 particles consisting of AS and succinic acid is lower than that of the well-mixed particles, while
314 experimental values for core-shell of AS/levoglucosan particles are close to those of the well-mixed
315 mixtures. The possible reasons for the difference between our study and results from Maskey et al.
316 (2014) are physical properties of the organic components, such as hygroscopicity, viscosity,
317 volatility, gas/liquid/solid diffusion coefficient of water vapor, and water uptake coefficients.
318 Thence, different kinds of organic compounds have a different effect in the hygroscopic growth of
319 mixtures, including the core-shell and the well-mixed state. For example, no hygroscopic growth
320 was observed up to 99 % RH for pure succinic acid particles (shown in Fig. S1a). Peng et al. (2001)
321 measured the DRH of succinic acid at 99% RH using a bulk solution at 24 °C. Also, Henning et al.
322 (2002) observed no hygroscopic growth factors of soot/succinic acid core-shell particles in the
323 hydration mode using a HTDMA. In the case of AS/succinic acid core-shell particles, No water
324 uptake by AS coated succinic acid shell was observed before 80% RH, while there is a gradual
325 increase in water absorption of core-shell particles prior to the deliquescence of AS with different
326 mass fraction of PA components as shown in Fig 5a-c. This suggested the physical state of shell is
327 solid and liquid for Maskey et al. (2014) and our measurements, respectively. At RH above 80%,
328 the kinetic limitation on the water vapor uptake through solid shell into the core is more obvious
329 than that through liquid shell into the core (i.e., liquid diffusion coefficient of water vapor is the
330 range of 10^{-10} to 10^{-9} , solid diffusion coefficient of water vapor is the range of 10^{-13} - 10^{-14} at 25°C).
331 This can lead to different hygroscopic behavior of core-shell particles. In the case of



332 AS/levoglucosan measured by Maskey et al. (2014), they found that the slightly higher growth
333 factors for the well-mixed particles is than core-shell aerosol particles (88nm AS core coating 12nm
334 levoglucosan). The mass fraction of levoglucosan in the core-shell particles is ~ 29wt %. In our
335 study, AS coated with PA with mass fraction range is between 46wt to 68wt %. Using the lower
336 mass fraction of PA (e.g., 29wt %), compared to mass fraction range of 46-68wt %, it may occur
337 lower hygroscopic growth factors of AS/PA core-shell particles than that of well mixed particles.
338 The low mass fraction of PA will be explored in future. In addition, by using the ZSR relation to
339 predict the hygroscopic growth factors of the internal mixture in the different mixing structures with
340 the same mass fractions of organic compounds, the measured growth factors of well-mixed AS/PA
341 particles agree well with the calculated growth factors by the ZSR relation comparing with that of
342 core-shell AS/PA particles.

343

344 **4 Summary and conclusion**

345 Due to different sources and aging process of aerosol particles in the atmosphere, atmospheric
346 aerosol particles tend to exist in different mixing structures, such as externally mixed, homogeneous
347 mixed (e.g., well-mixed and core-shell structure). In this work, PA is used as a representative organic
348 component generated from various sources, such as vehicles, biomass burning, photo-oxidation to
349 investigate hygroscopic behavior of AS/PA aerosol particles with different mixing states.
350 Continuous water absorption by pure PA aerosol particles has an important contribution in
351 smoothing of hygroscopic curve of AS/PA well-mixed mixtures with increasing mass fraction of PA
352 components. In addition, the ZSR relation is a good estimation of experimental hygroscopic growth
353 factors of AS/PA well-mixed particles. Furthermore, A coating-HTDMA technique study on the PA



354 coating effects on the hygroscopicity of AS core is investigated. PA coating increase the water
355 uptake by core-shell at RH prior to the AS deliquescence but decrease hygroscopic growth of core-
356 shell particles at high RH. Finally, we and compared and discussed the difference of influence of
357 mixing structures on the hygroscopicity of AS/PA aerosol particles. In addition, in this study, using
358 an E-AIM model, Fitted Expression Eq. (1), and the ZSR relation is to predict the measured
359 hygroscopic growth factors of pure components, well-mixed, and core-shell particles, respectively.
360 According to filed studies reported in the previous literature, a variety of organic aerosol particles
361 were characterized in the atmosphere. Thence, the effect of various organic substances on the
362 hygroscopic behavior cycle of the organic/inorganic core-shell particles need to be further
363 investigated. Currently, suppression or delay of the DRH and ERH of core-shell particles to some
364 extent depends on the different types of organic compound coatings, such as molecular structure,
365 viscosity, solubility and hygroscopicity. Also, for the certain organic compounds such as PA, a
366 difference in the hygroscopic behavior of mixing states is more likely to depend on the difference
367 of influence of kinetic limitations. Moreover, in order to understand which models suitable to
368 explain these potential atmospheric relevant core-shell aerosol hygroscopicities, and whether they
369 contain any rules related to functional groups of the organic components, it is significant to explore
370 the possibility of modeling combining with the experimental measurements. Understanding the
371 contribution of different organics coating to hygroscopic behavior of the core-shell mixtures as well
372 as discussion of the extent to which kinetic limitations or organic physico-chemical properties is
373 expected to have contributed to difference in the hygroscopicity in the different mixing structure,
374 which may lead toward a more mechanistic understanding of how water uptake can be linked to the
375 mixing states in the atmosphere.



376 This work focus on the water uptake by these aerosol particles in the different mixing states.
377 Atmospheric aerosol particles may undergo the humidity cycles depend on the ambient RH history.
378 A hysteresis effect with solid-liquid phase transition of core-shell aerosol particles may occur as RH
379 decreases in the ambient air. Also, more attention to the residence time will be paid on core-shell
380 aerosol particles to reach equilibrium in the whole of RH range. These changes related to the
381 hygroscopic behavior of core-shell aerosol particles studies will be a topic in the future.

382

383 **Author contributions:** W.G.W designed and led the study. W.G.W and T.L assembled the
384 coating-HTDMA. T.L performed the experiments and prepared the manuscript with contributions
385 from all co-authors. All co-authors discussed the results and commented on manuscript.

386 **Data availability**

387 The data used in this study are available upon request from the corresponding author.

388 **Acknowledgement**

389 This project was supported by The National Key Research and Development Program of China
390 (2017YFC0209500), and the National Natural Science Foundation of China (41822703, 91744204,
391 91844301).

392

393 **Reference**

394 Abo Riziq, A., Trainic, M., Erlick, C., Segre, E., and Rudich, Y.: Extinction efficiencies of coated
395 absorbing aerosols measured by cavity ring down aerosol spectrometry, *Atmos. Chem. Phys.*, 8,
396 1823-1833, 2008.

397 Abo Riziq, A., Erlick, C., Dinar, E., and Rudich, Y.: Optical properties of absorbing and non-



398 absorbing aerosols retrieved by cavity ring down (CRD) spectroscopy, *Atmos. Chem. Phys.*, 7,
399 1523-1536, 2007.

400 Ansari, A. S. and Pandis, S. N.: Water Absorption by Secondary Organic Aerosol and Its Effect on
401 Inorganic Aerosol Behavior, *Environmental Science & Technology*, 34, 71-77, 2000.

402 Bertram, A. K., Martin, S. T., Hanna, S. J., Smith, M. L., Bodsworth, A., Chen, Q., Kuwata, M., Liu,
403 A., You, Y., and Zorn, S. R.: Predicting the relative humidities of liquid-liquid phase separation,
404 efflorescence, and deliquescence of mixed particles of ammonium sulfate, organic material, and
405 water using the organic-to-sulfate mass ratio of the particle and the oxygen-to-carbon elemental
406 ratio of the organic component, *Atmos. Chem. Phys.*, 11, 10995-11006, 2011.

407 Brooks, S. D., DeMott, P. J., and Kreidenweis, S. M.: Water uptake by particles containing humic
408 materials and mixtures of humic materials with ammonium sulfate, *Atmospheric Environment*, 38,
409 1859-1868, 2004.

410 Chan, M. N., Lee, A. K. Y., and Chan, C. K.: Responses of ammonium sulfate particles coated with
411 glutaric acid to cyclic changes in relative humidity: Hygroscopicity and Raman characterization,
412 *Environmental Science & Technology*, 40, 6983-6989, 2006.

413 Cheng, Y. F., Wiedensohler, A., Eichler, H., Heintzenberg, J., Tesche, M., Ansmann, A., Wendisch,
414 M., Su, H., Althausen, D., Herrmann, H., Gnauk, T., Brüggemann, E., Hu, M., and Zhang, Y. H.:
415 Relative humidity dependence of aerosol optical properties and direct radiative forcing in the surface
416 boundary layer at Xinken in Pearl River Delta of China: An observation based numerical study,
417 *Atmospheric Environment*, 42, 6373-6397, 2008.

418 Choi, M. Y. and Chan, C. K.: The Effects of Organic Species on the Hygroscopic Behaviors of
419 Inorganic Aerosols, *Environmental Science & Technology*, 36, 2422-2428, 2002.



- 420 Ciobanu, V. G., Marcolli, C., Krieger, U. K., Weers, U., and Peter, T.: Liquid–Liquid Phase
421 Separation in Mixed Organic/Inorganic Aerosol Particles, *The Journal of Physical Chemistry A*, 113,
422 10966-10978, 2009.
- 423 Cruz, C. N. and Pandis, S. N.: Deliquescence and Hygroscopic Growth of Mixed Inorganic–Organic
424 Atmospheric Aerosol, *Environmental Science & Technology*, 34, 4313-4319, 2000.
- 425 Eichler, H., Cheng, Y. F., Birmili, W., Nowak, A., Wiedensohler, A., Brüggemann, E., Gnauk, T.,
426 Herrmann, H., Althausen, D., Ansmann, A., Engelmann, R., Tesche, M., Wendisch, M., Zhang, Y.
427 H., Hu, M., Liu, S., and Zeng, L. M.: Hygroscopic properties and extinction of aerosol particles at
428 ambient relative humidity in South-Eastern China, *Atmospheric Environment*, 42, 6321-6334, 2008.
- 429 Falkovich, A. H., Schkolnik, G., Ganor, E., and Rudich, Y.: Adsorption of organic compounds
430 pertinent to urban environments onto mineral dust particles, *Journal of Geophysical Research:*
431 *Atmospheres*, 109, n/a-n/a, 2004.
- 432 Ganguly, D., Jayaraman, A., Rajesh, T. A., and Gadhavi, H.: Wintertime aerosol properties during
433 foggy and nonfoggy days over urban center Delhi and their implications for shortwave radiative
434 forcing, *Journal of Geophysical Research: Atmospheres*, 111, 2006.
- 435 Garland, R. M., Wise, M. E., Beaver, M. R., DeWitt, H. L., Aiken, A. C., Jimenez, J. L., and Tolbert,
436 M. A.: Impact of palmitic acid coating on the water uptake and loss of ammonium sulfate particles,
437 *Atmos. Chem. Phys.*, 5, 1951-1961, 2005.
- 438 Gupta, D., Kim, H., Park, G., Li, X., Eom, H. J., and Ro, C. U.: Hygroscopic properties of NaCl and
439 NaNO₃ mixture particles as reacted inorganic sea-salt aerosol surrogates, *Atmos.*
440 *Chem. Phys.*, 15, 3379-3393, 2015.
- 441 Hämeri, K., Charlson, R., and Hansson, H.-C.: Hygroscopic properties of mixed ammonium sulfate



442 and carboxylic acids particles, *AIChE Journal*, 48, 1309-1316, 2002.

443 Heintzenberg, J., Maßling, A., and Birmili, W.: The connection between hygroscopic and optical
444 particle properties in the atmospheric aerosol, *Geophysical Research Letters*, 28, 3649-3651, 2001.

445 Hodas, N., Zuend, A., Mui, W., Flagan, R., and Seinfeld, J.: Influence of particle-phase state on the
446 hygroscopic behavior of mixed organic-inorganic aerosols, *Atmospheric Chemistry and Physics*,
447 15, 5027-5045, 2015.

448 Hori, M., Ohta, S., Muraio, N., and Yamagata, S.: Activation capability of water soluble organic
449 substances as CCN, *Journal of Aerosol Science*, 34, 419-448, 2003.

450 Huff Hartz, K. E., Tischuk, J. E., Chan, M. N., Chan, C. K., Donahue, N. M., and Pandis, S. N.:
451 Cloud condensation nuclei activation of limited solubility organic aerosol, *Atmospheric*
452 *Environment*, 40, 605-617, 2006.

453 Jing, B., Tong, S., Liu, Q., Li, K., Wang, W., Zhang, Y., and Ge, M.: Hygroscopic behavior of
454 multicomponent organic aerosols and their internal mixtures with ammonium sulfate, *Atmospheric*
455 *Chemistry and Physics*, 16, 4101-4118, 2016.

456 K., C. M. N. a. C. C.: Mass transfer effects in hygroscopic measurements of aerosol particles,
457 *Atmospheric Chemistry and Physics*, 2005. 2005.

458 Kawamura, K. and Ikushima, K.: Seasonal changes in the distribution of dicarboxylic acids in the
459 urban atmosphere, *Environmental Science & Technology*, 27, 2227-2235, 1993.

460 Kreidenweis, S. M., Koehler, K., DeMott, P. J., Prenni, A. J., Carrico, C., and Ervens, B.: Water
461 activity and activation diameters from hygroscopicity data - Part I: Theory and application to
462 inorganic salts, *Atmospheric Chemistry and Physics*, 5, 1357-1370, 2005.

463 Lang-Yona, N., Abo-Riziq, A., Erlick, C., Segre, E., Trainic, M., and Rudich, Y.: Interaction of



464 internally mixed aerosols with light, *Physical Chemistry Chemical Physics*, 12, 21-31, 2010.

465 Lei, T., Zuend, A., Cheng, Y., Su, H., Wang, W., and Ge, M.: Hygroscopicity of organic surrogate
466 compounds from biomass burning and their effect on the efflorescence of ammonium
467 sulfate in mixed aerosol particles, *Atmos. Chem. Phys.*, 18, 1045-1064, 2018.

468 Lei, T., Zuend, A., Wang, W. G., Zhang, Y. H., and Ge, M. F.: Hygroscopicity of organic compounds
469 from biomass burning and their influence on the water uptake of mixed organic ammonium sulfate
470 aerosols, *Atmospheric Chemistry and Physics*, 14, 1-20, 2014.

471 Lesins, G., Chylek, P., and Lohmann, U.: A study of internal and external mixing scenarios and its
472 effect on aerosol optical properties and direct radiative forcing, *Journal of Geophysical Research:*
473 *Atmospheres*, 107, AAC 5-1-AAC 5-12, 2002.

474 Liu, Q., Jing, B., Peng, C., Tong, S., Wang, W., and Ge, M.: Hygroscopicity of internally mixed
475 multi-component aerosol particles of atmospheric relevance, *Atmospheric Environment*, 125, 69-
476 77, 2016.

477 Liu, X., Gu, J., Li, Y., Cheng, Y., Qu, Y., Han, T., Wang, J., Tian, H., Chen, J., and Zhang, Y.: Increase
478 of aerosol scattering by hygroscopic growth: Observation, modeling, and implications on visibility,
479 *Atmospheric Research*, 132, 91-101, 2013.

480 Liu, X., Zhang, Y., Cheng, Y., Hu, M., and Han, T.: Aerosol hygroscopicity and its impact on
481 atmospheric visibility and radiative forcing in Guangzhou during the 2006 PRIDE-PRD campaign,
482 *Atmospheric Environment*, 60, 59-67, 2012.

483 Martin, A. C., Cornwell, G. C., Atwood, S. A., Moore, K. A., Rothfuss, N. E., Taylor, H., DeMott,
484 P. J., Kreidenweis, S. M., Petters, M. D., and Prather, K. A.: Transport of pollution to a remote
485 coastal site during gap flow from California's interior: impacts on aerosol composition, clouds, and



486 radiative balance, *Atmos. Chem. Phys.*, 17, 1491-1509, 2017.

487 Maskey, S., Chong, K. Y., Kim, G., Kim, J.-S., Ali, A., and Park, K.: Effect of mixing structure on
488 the hygroscopic behavior of ultrafine ammonium sulfate particles mixed with succinic acid and
489 levoglucosan, *Particuology*, 13, 27-34, 2014.

490 Miñambres, L., Sánchez, M. N., Castaño, F., and Basterretxea, F. J.: Hygroscopic Properties of
491 Internally Mixed Particles of Ammonium Sulfate and Succinic Acid Studied by Infrared
492 Spectroscopy, *The Journal of Physical Chemistry A*, 114, 6124-6130, 2010.

493 Pagels, J., Khalizov, A. F., McMurry, P. H., and Zhang, R. Y.: Processing of Soot by Controlled
494 Sulphuric Acid and Water Condensation—Mass and Mobility Relationship, *Aerosol Science and
495 Technology*, 43, 629-640, 2009.

496 Peng, C., Chan, M. N., and Chan, C. K.: The Hygroscopic Properties of Dicarboxylic and
497 Multifunctional Acids: Measurements and UNIFAC Predictions, *Environmental Science &
498 Technology*, 35, 4495-4501, 2001.

499 Qiu, C. and Zhang, R.: Multiphase chemistry of atmospheric amines, *Physical Chemistry Chemical
500 Physics*, 15, 5738-5752, 2013.

501 Rogge, W. F., Mazurek, M. A., Hildemann, L. M., Cass, G. R., and Simoneit, B. R. T.: Quantification
502 of urban organic aerosols at a molecular level: Identification, abundance and seasonal variation,
503 *Atmospheric Environment. Part A. General Topics*, 27, 1309-1330, 1993.

504 Rose, D., Gunthe, S. S., Su, H., Garland, R. M., Yang, H., Berghof, M., Cheng, Y. F., Wehner, B.,
505 Achtert, P., Nowak, A., Wiedensohler, A., Takegawa, N., Kondo, Y., Hu, M., Zhang, Y., Andreae, M.
506 O., and Pöschl, U.: Cloud condensation nuclei in polluted air and biomass burning smoke near the
507 mega-city Guangzhou, China -Part 2: Size-resolved aerosol chemical composition, diurnal cycles,



508 and externally mixed weakly CCN-active soot particles, *Atmospheric Chemistry and Physics*, 11,
509 2817-2836, 2011.

510 Rudich, Y.: Laboratory Perspectives on the Chemical Transformations of Organic Matter in
511 Atmospheric Particles, *Chemical Reviews*, 103, 5097-5124, 2003.

512 Saxena, P., Hildemann, L. M., McMurry, P. H., and Seinfeld, J. H.: Organics alter hygroscopic
513 behavior of atmospheric particles, *Journal of Geophysical Research: Atmospheres*, 100, 18755-
514 18770, 1995.

515 Schauer, J. J. and Cass, G. R.: Source Apportionment of Wintertime Gas-Phase and Particle-Phase
516 Air Pollutants Using Organic Compounds as Tracers, *Environmental Science & Technology*, 34,
517 1821-1832, 2000.

518 Schauer, J. J., Fraser, M. P., Cass, G. R., and Simoneit, B. R. T.: Source Reconciliation of
519 Atmospheric Gas-Phase and Particle-Phase Pollutants during a Severe Photochemical Smog
520 Episode, *Environmental Science & Technology*, 36, 3806-3814, 2002.

521 Schauer, J. J., Rogge, W. F., Hildemann, L. M., Mazurek, M. A., Cass, G. R., and Simoneit, B. R.
522 T.: Source apportionment of airborne particulate matter using organic compounds as tracers,
523 *Atmospheric Environment*, 30, 3837-3855, 1996.

524 Schwarz, J. P., Gao, R. S., Fahey, D. W., Thomson, D. S., Watts, L. A., Wilson, J. C., Reeves, J. M.,
525 Darbeheshti, M., Baumgardner, D. G., Kok, G. L., Chung, S. H., Schulz, M., Hendricks, J., Lauer,
526 A., Kärcher, B., Slowik, J. G., Rosenlof, K. H., Thompson, T. L., Langford, A. O., Loewenstein, M.,
527 and Aikin, K. C.: Single-particle measurements of midlatitude black carbon and light-scattering
528 aerosols from the boundary layer to the lower stratosphere, *Journal of Geophysical Research:*
529 *Atmospheres*, 111, n/a-n/a, 2006.



- 530 Shi, Y. J., Ge, M. F., and Wang, W. G.: Hygroscopicity of internally mixed aerosol particles
531 containing benzoic acid and inorganic salts, *Atmospheric Environment*, 60, 9-17, 2012.
- 532 Shiraiwa, M., Zuend, A., Bertram, A. K., and Seinfeld, J. H.: Gas-particle partitioning of
533 atmospheric aerosols: interplay of physical state, non-ideal mixing and morphology, *Physical*
534 *Chemistry Chemical Physics*, 15, 11441-11453, 2013.
- 535 Sjogren, S., Gysel, M., Weingartner, E., Baltensperger, U., Cubison, M. J., Coe, H., Zardini, A. A.,
536 Marcolli, C., Krieger, U. K., and Peter, T.: Hygroscopic growth and water uptake kinetics of two-
537 phase aerosol particles consisting of ammonium sulfate, adipic and humic acid mixtures, *Journal of*
538 *Aerosol Science*, 38, 157-171, 2007.
- 539 Song, M., Ham, S., Andrews, R. J., You, Y., and Bertram, A. K.: Liquid-liquid phase separation in
540 organic particles containing one and two organic species: importance of the average
541 O/C , *Atmos. Chem. Phys.*, 18, 12075-12084, 2018.
- 542 Song, M., Marcolli, C., Krieger, U. K., Zuend, A., and Peter, T.: Liquid-liquid phase separation and
543 morphology of internally mixed dicarboxylic acids/ammonium sulfate/water particles, *Atmospheric*
544 *Chemistry and Physics*, 12, 2691-2712, 2012a.
- 545 Song, M., Marcolli, C., Krieger, U. K., Zuend, A., and Peter, T.: Liquid-liquid phase separation in
546 aerosol particles: Dependence on O/C , organic functionalities, and compositional complexity,
547 *Geophysical Research Letters*, 39, 2012b.
- 548 Spindler, C., Riziq, A. A., and Rudich, Y.: Retrieval of Aerosol Complex Refractive Index by
549 Combining Cavity Ring Down Aerosol Spectrometer Measurements with Full Size Distribution
550 Information, *Aerosol Science and Technology*, 41, 1011-1017, 2007.
- 551 Stock, M., Cheng, Y. F., Birmili, W., Massling, A., Wehner, B., Müller, T., Leinert, S., Kalivitis, N.,



- 552 Mihalopoulos, N., and Wiedensohler, A.: Hygroscopic properties of atmospheric aerosol particles
553 over the Eastern Mediterranean: implications for regional direct radiative forcing under clean and
554 polluted conditions, *Atmos. Chem. Phys.*, 11, 4251-4271, 2011.
- 555 Su, H., Rose, D., Cheng, Y. F., Gunthe, S. S., Massling, A., Stock, M., Wiedensohler, A., Andreae,
556 M. O., and Pöschl, U.: Hygroscopicity distribution concept for measurement data analysis and
557 modeling of aerosol particle mixing state with regard to hygroscopic growth and CCN activation,
558 *Atmos. Chem. Phys.*, 10, 7489-7503, 2010.
- 559 Tie, X., Huang, R.-J., Cao, J., Zhang, Q., Cheng, Y., Su, H., Chang, D., Pöschl, U., Hoffmann, T.,
560 Dusek, U., Li, G., Worsnop, D. R., and O'Dowd, C. D.: Severe Pollution in China Amplified by
561 Atmospheric Moisture, *Scientific Reports*, 7, 15760, 2017.
- 562 Wang, G., Kawamura, K., Xie, M., Hu, S., Li, J., Zhou, B., Cao, J., and An, Z.: Selected water-
563 soluble organic compounds found in size-resolved aerosols collected from urban, mountain and
564 marine atmospheres over East Asia, *Tellus B*, 63, 371-381, 2011.
- 565 Wex, H., Hennig, T., Salma, I., Ocskay, R., Kiselev, A., Henning, S., Massling, A., Wiedensohler,
566 A., and Stratmann, F.: Hygroscopic growth and measured and modeled critical super-saturations of
567 an atmospheric HULIS sample, *Geophysical Research Letters*, 34, n/a-n/a, 2007.
- 568 Xue, H., Khalizov, A. F., Wang, L., Zheng, J., and Zhang, R.: Effects of dicarboxylic acid coating
569 on the optical properties of soot, *Physical Chemistry Chemical Physics*, 11, 7869-7875, 2009.
- 570 You, Y., Smith, M. L., Song, M., Martin, S. T., and Bertram, A. K.: Liquid-liquid phase separation
571 in atmospherically relevant particles consisting of organic species and inorganic salts, *International*
572 *Reviews in Physical Chemistry*, 33, 43-77, 2014.
- 573 Zamora, I. R., Tabazadeh, A., Golden, D. M., and Jacobson, M. Z.: Hygroscopic growth of common



574 organic aerosol solutes, including humic substances, as derived from water activity measurements,
575 Journal of Geophysical Research: Atmospheres, 116, n/a-n/a, 2011.

576 Zawadowicz, M. A., Proud, S. R., Seppalainen, S. S., and Cziczo, D. J.: Hygroscopic and phase
577 separation properties of ammonium sulfate/organics/water ternary solutions, Atmos. Chem. Phys.,
578 15, 8975-8986, 2015.

579 Zelenyuk, A., Cai, Y., and Imre, D.: From Agglomerates of Spheres to Irregularly Shaped Particles:
580 Determination of Dynamic Shape Factors from Measurements of Mobility and Vacuum
581 Aerodynamic Diameters, Aerosol Science and Technology, 40, 197-217, 2006.

582 Zhang, Q., Canagaratna, M. R., Jayne, J. T., Worsnop, D. R., and Jimenez, J.-L.: Time- and size-
583 resolved chemical composition of submicron particles in Pittsburgh: Implications for aerosol
584 sources and processes, Journal of Geophysical Research: Atmospheres, 110, n/a-n/a, 2005.

585 Zhang, R., Khalizov, A. F., Pagels, J., Zhang, D., Xue, H., and McMurry, P. H.: Variability in
586 morphology, hygroscopicity, and optical properties of soot aerosols during atmospheric processing,
587 Proceedings of the National Academy of Sciences, 105, 10291-10296, 2008.

588 Zhang, Y.-L., Kawamura, K., Watanabe, T., Hatakeyama, S., Takami, A., and Wang, W.: New
589 directions: Need for better understanding of source and formation process of phthalic acid in
590 aerosols as inferred from aircraft observations over China, Atmospheric Environment, 140, 147-149,
591 2016.

592 Zhou, Q., Pang, S.-F., Wang, Y., Ma, J.-B., and Zhang, Y.-H.: Confocal Raman Studies of the
593 Evolution of the Physical State of Mixed Phthalic Acid/Ammonium Sulfate Aerosol Droplets and
594 the Effect of Substrates, The Journal of Physical Chemistry B, 118, 6198-6205, 2014.

595 Zuend, A., Marcolli, C., Luo, B. P., and Peter, T.: A thermodynamic model of mixed organic-



596 inorganic aerosols to predict activity coefficients, Atmospheric Chemistry and Physics, 8, 4559-
597 4593, 2008.

598 Zuend, A., Marcolli, C., Peter, T., and Seinfeld, J. H.: Computation of liquid-liquid equilibria and
599 phase stabilities: implications for RH-dependent gas/particle partitioning of organic-inorganic
600 aerosols, Atmospheric Chemistry and Physics, 10, 7795-7820, 2010.

601 Zuend, A. and Seinfeld, J. H.: A practical method for the calculation of liquid-liquid equilibria in
602 multicomponent organic-water-electrolyte systems using physicochemical constraints, Fluid Phase
603 Equilibria, 337, 201-213, 2013.

604

605

606

607

608

609

610

611

612

613

614

615

616

617



618

619 **Tables**

620 **Table 1.** Coefficients of the fitted growth curve parameterization to measured growth
621 factor data using Eq. (1)

Chemical Compound	a	b	c
Phthalic Acid	0.083116	0.291473	-0.353544

622

623

624

625

626

627

628

629

630

631

632

633

634

635

636

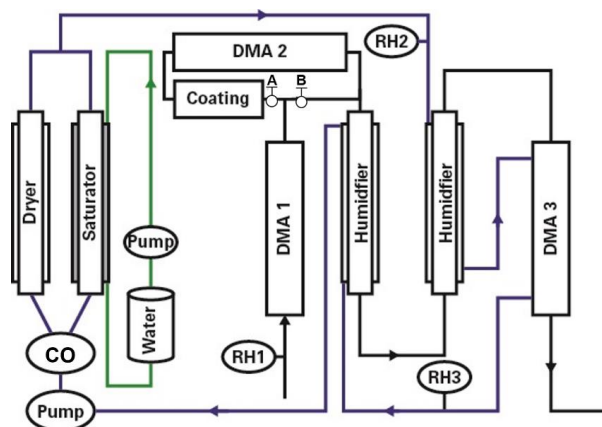
637



638

639 **Figures**

640



641

642 **Figure 1.** Schematic diagram of the coating-hygroscopicity tandem differential mobility analyzer. Here,

643 CO: critical orifice; DMA: differential mobility analyzer; RH1 and RH2 (measured RH sensor) represent

644 the RH of aerosol and humidified flow in the inlet of DMA1 and humidifier, respectively. RH3 (measured

645 by dew point mirror) represent the RH of excess air. Valve B is open and valve A is closed to the

646 homogeneous internally mixed-mode experiment. Valve A is open and Valve B is closed to the coating-

647 mode experiment. Black line: aerosol line; Blue line: sheath line; Green line: MilliQ water.

648

649

650

651

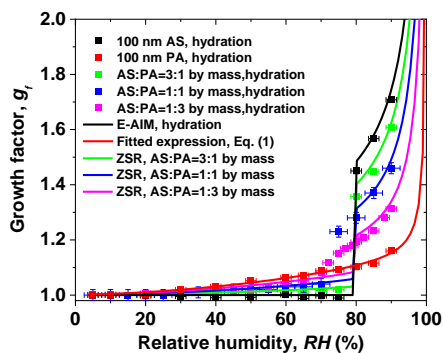
652

653

654



655



656

657 **Figure 2.** Hygroscopic growth factor for 100 nm (dry diameter, $RH < 5\%$) aerosol particles containing:
658 ammonium sulfate (AS), phthalic acid (PA), and well-mixed mixtures of PA and AS with different mass
659 ratio of AS to PA. In comparison, the E-AIM model, the Fitted expression Eq. (1), and the ZSR relation
660 predicted growth factors of AS, PA, and well mixed particles with different mass fractions of PA,
661 respectively.

662

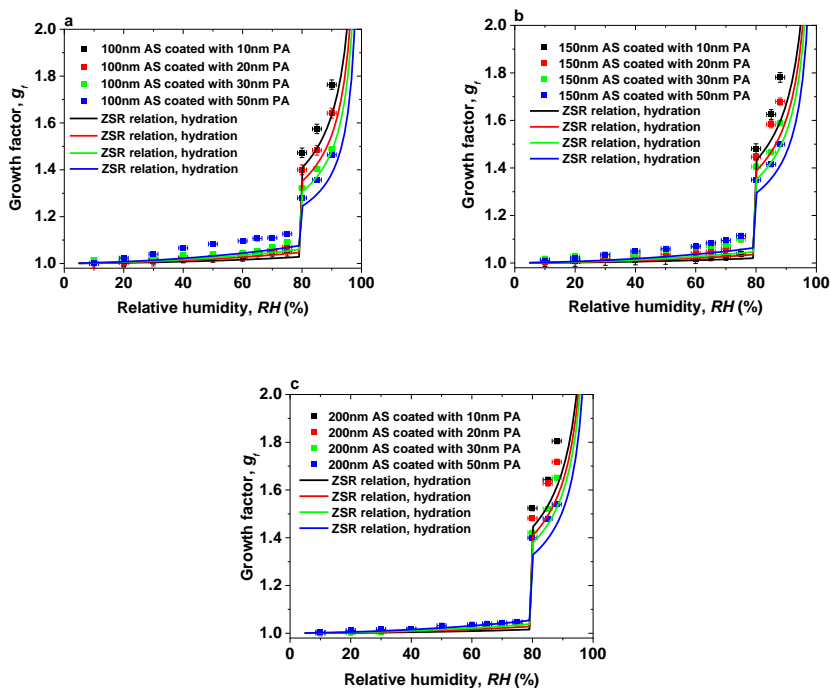
663

664

665

666

667



668

669

670 **Figure 3.** Hygroscopic growth factor for core-shell of ammonium sulfate (AS) and phthalic acid (PA)

671 aerosol particles. In comparison, the ZSR relation predicted growth factor of core-shell aerosol particles

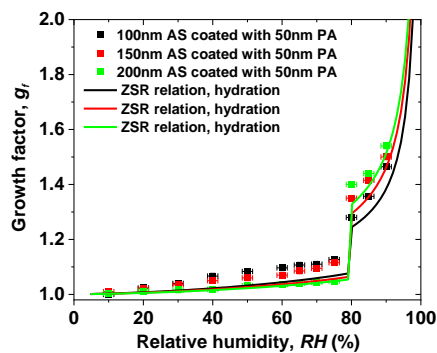
672 (a) 100-nm AS core (b) 150-nm AS core (c) 200-nm AS core.

673

674

675

676



677

678 **Figure 4.** Hygroscopic growth factor for 100-200 nm ammonium sulfate (AS) core with coating 50 nm

679 phthalic acid (PA). In comparison, the ZSR relation predicted growth factor of core-shell aerosol particles

680 with different AS cores.

681

682

683

684

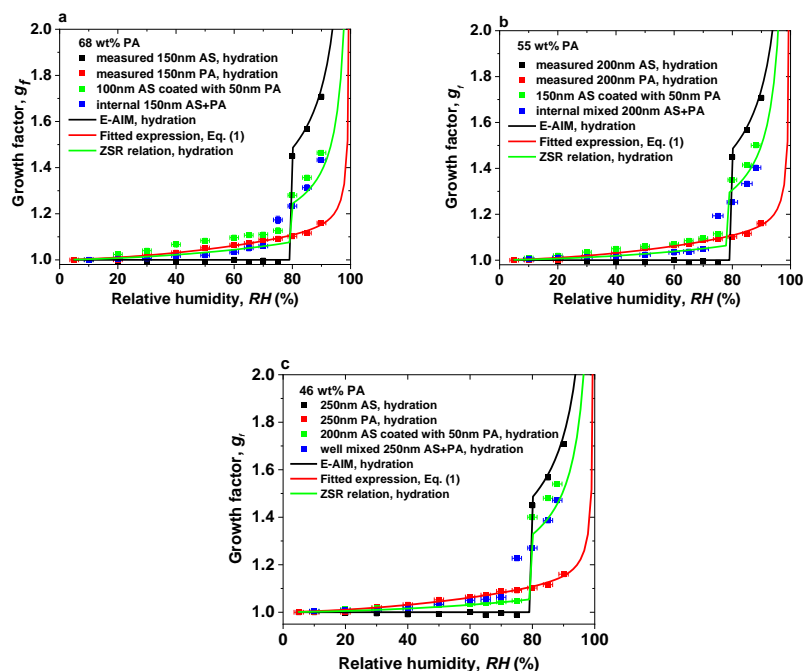
685

686

687

688

689



690

691

692

693 **Figure 5.** Hygroscopic growth factor for core-shell and well-mixed aerosol particles with the same dry
694 mass fractions of phthalic acid (PA) containing: (a): 68 wt % PA, (b): 55 wt % PA, (c): 46 wt % PA. In
695 comparison, the E-AIM model, the Fitted expression Eq. (1), and the ZSR relation predicted growth
696 factors of ammonium sulfate (AS), PA, and internally mixed particles with different mass fractions of
697 PA, respectively.

698

699

700

701

702